Flyby dynamical characterisation with Jacobian eigenvalues

Alessandro Masat*[1], Camilla Colombo†[1], and Arnaud Boutonnet‡[2]

[1]Politecnico di Milano, Milano, Italy, 20156
[2]European Space Agency (ESA-ESOC), Darmstadt, Germany, 64293

1 Introduction

The detection of flybys in the numerical propagation of interplanetary trajectories is a key aspect to enable planetary protection analyses. Their much faster dynamics, compared to the pure heliocentric motion, hinders the development of advanced orbital integrators: regularisation-based approaches and variation of parameters implementations are extremely sensitive on close approach events, and may fail in correctly predicting their effect on the propagated trajectory. Switching the integration/regularisation centre to the flyby body in case of close approaches is an effective workaround to retain all the benefits of advanced propagation techniques [1]. Nonetheless, this philosophy requires to properly define and, consequently, detect possible flyby events.

The commonly used concepts all rely on the definition of a spherical region that surrounds any solar system planet. In general, the stronger the gravitational field of the minor body, the larger its associated sphere. *Sphere of influence* (SOI) and *Hill's sphere* are the two usually adopted definitions. The former approximates the distance from the minor body where either the planet or the Sun can be considered as a perturbation of the other dynamics. The latter approximates the distance of the Lagrange points L_1 and L_2 from the planet [3]. Differently from these definitions, Debatin et al. [2] used the eigenvalues of the dynamics' Jacobian to measure the relative magnitudes of the contribution of the different bodies in an N-body system, and used it as robust step control mechanism. Similarly, Romano [5] used this criterion to detect flybys in planetary protection analyses.

This work analyses flybys from a different perspective. Rather than building on a concept based on equilibrium distances, the dynamical nature of the close approach is emphasised. The eigenvalues of the three-body problem dynamics' Jacobian leads to an analytical solution for a spheroidal locus of points that locally highlights which body is contributing the most to the dynamics variation. The results are also compared against the Circular Restricted Three-Body Problem (CR3BP) zero-velocity curves concept.

2 Jacobian eigenvalues for flyby detection

The dynamics' Jacobian is traditionally linked to the step size control for general numerical simulations. In particular, the maximum eigenvalue influences the stability of the numerical scheme [4]. Contrarily to predictor-corrector integrators (e.g. the Runge-Kutta family), the knowledge on the dynamics Jacobian is exploited to minimise the truncation error. In the orbital dynamics case, the work of Debatin et al. [2] used an analytical approximation of the maximum Jacobian eigenvalue of the N-body dynamics, building a fast integration algorithm with step size control. They approximate the square of the maximum Jacobian eigenvalue λ^2_{max} as the sum of the squares of all the separate two-body Jacobian eigenvalues:

$$\lambda^2_{max} \approx \sum_{i=1}^{N} \lambda_i^2 = \sum_{i=1}^{N} \frac{2\mu_i}{\left|\mathbf{r} - \mathbf{r}_i\right|^3} \tag{1}$$

with the subscript i denoting the i-th body, $\mathbf{r}$ the position and μ_i the gravitational parameter. This approximation becomes particularly reliable far from the boundaries of any sphere of influence/Hill's sphere, since in these regions either the Sun or the planet flown by heavily dominates the dynamics.

The later work of Romano [5] used a similar approximation approach to implement a flyby detection criterion. If the ratio between the eigenvalues of a given planet and the Sun grows above a user-specified tolerance, then a flyby event is detected. Romano also showed that this criterion encompasses the usually defined sphere of influence/Hill's sphere, in the case of threshold set equal to 1.

3 Dynamical meaning in the Three-body problem

The barycentric three-body Jacobian $\mathbf{J}$ is defined as:

$$\mathbf{J} = \begin{bmatrix} \mathbf{0} & \mathbf{I} \\ \mathbf{G} & \mathbf{0} \end{bmatrix} \tag{2}$$

*Email: alessandro.masat@polimi.it. PhD Candidate, Department of Aerospace Science and Technology.
†Email: camilla.colombo@polimi.it. Associate Professor, Department of Aerospace Science and Technology.
‡Email: arnaud.boutonnet@esa.int. Senior Mission Analyst, HSO-GFA, ESA-ESOC.

with $\mathbf{0}$ and $\mathbf{I}$ the 3×3 null and identity matrices, respectively, and $\mathbf{G}$ defined as:

$$\mathbf{G} = \sum_{i=1}^{2} \mathbf{G}_i = \sum_{i=1}^{2} \frac{\mu_i}{|\mathbf{d}_i|^5} \left(|\mathbf{d}_i|^2 \mathbf{I} - 3\mathbf{d}_i \mathbf{d}_i^T \right) \quad (3)$$

with $\mathbf{d}_i = \mathbf{r} - \mathbf{r}_i$. It can be proved that, in the two-body case, $\lambda_{j,\mathbf{J}} \equiv \lambda^2_{j,\mathbf{G}}$, with $j = 1, 2, 3$, and $\lambda^2_{max,\mathbf{G}}$ is defined as in Equation (1) [5]. λ^2 appears only on the right-hand side because the properties of the determinant of block-square matrices are introduced to compute the eigenvalues of $\mathbf{J}$.

Approximating the dynamics as if only the currently dominant body 1 was present reflects on the approximated Jacobian as $\mathbf{G} \approx \mathbf{G}_1$. The matrix Jacobian error becomes equal to $\mathbf{G}_2$. Since any $\mathbf{G}_i$ is symmetric (Equation (3)), its euclidean matrix norm equals its spectral radius, i.e. $|\mathbf{G}_i|_2 \equiv \rho(\mathbf{G}_i) \equiv \lambda_{max,\mathbf{G}_i}$. In other words, the maximum eigenvalue of $\mathbf{G}_2$ directly measures the error of $\mathbf{G} \approx \mathbf{G}_1$.

The color scale in Figure 1 shows the maximum Jacobian error values in the space near Jupiter, i.e. $\max\left[\lambda_{max,Sun}/\lambda_{max}, \lambda_{max,Jup}/\lambda_{max}\right]$, on the plane containing Jupiter's orbit about the Sun. Rather than crossing a fixed-shape spheroid, the proposed visualisation highlights the smooth transition nature of flybys. Even if fast, the whole continuous domain is crossed, starting from the interplanetary space, passing through a region where none of the two bodies dominates the gravitational acceleration change, and finally reaching a far greater planetary effect at low altitudes. Two higher error regions, called "Thickened regions" in Figure 1, appear nearly perpendicularly to the Sun-Jupiter direction. The possible reason of their appearence is explored in Section 5.

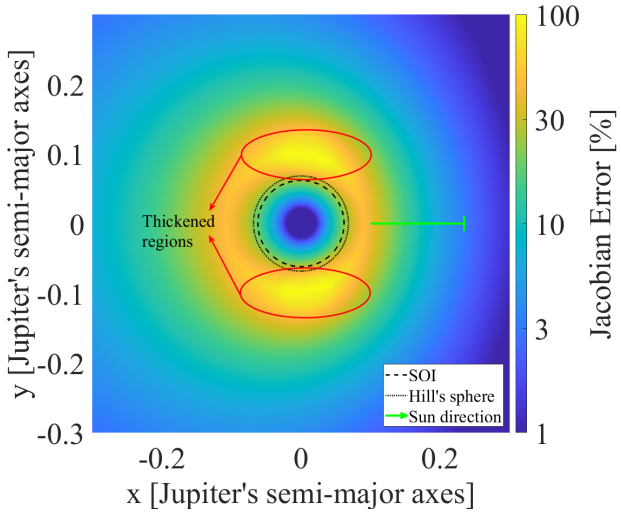

Figure 1: Jupiter's Jacobian percent error (color scale), compared against Hill's surfaces (dotted) and SOI (dashed).

Equivalently, this criterion highlights the highest curvature regions of the three-body gravitational potential $V = -\mu_1/|\mathbf{d}_1| - \mu_2/|\mathbf{d}_2|$, since it can be proved that $\mathbf{G} \equiv Hessian(V)$. In other words, the space regions determining a flyby may be identified by the local curvature of the gravitational potential.

4 Analytical loci of points

Replacing the $\mathbf{G}, \mathbf{J}$ subscript notation with the body names, a direct comparison can be made with the parametrisation $\lambda_{max,Jup}/\lambda_{max,Sun} = \gamma$. As done in Figure 1, centering the reference frame on Jupiter leads to an analytical expression for the spheroidal loci with common γ, whose radius $\tilde{r}$ is:

$$\tilde{r}(\theta) = r_{Sun-Jup} \frac{-\alpha \cos\theta + \sqrt{\alpha(1 - \alpha \sin^2\theta)}}{1 - \alpha} \quad (4)$$

with θ the angle between the direction of $\tilde{r}$ and the direction identified by the line connecting the Sun and Jupiter, and $\alpha = (\gamma \mu_{Jup}/\mu_{Sun})^{2/3}$. The $2/3$ exponent arises because of the third power of the eigenvalue expression (Equation (1)), and a squaring taken to remove the square root of the vector norm operator.

Figure 2 extends Figure 1, comparing the analytical loci of points obtained with Equation (4) against the computed values of the Jacobian error (on the color scale), for γ equal to 0.1, 1, and 10. The cases $\gamma = 0.1, 10$ (dashed red lines) well bound the regions where the Jacobian approximation error is higher than 10%. Thickened regions aside, the case $\gamma = 1$ (solid red line) perfectly predicts the "critical" distances where the error is maximised.

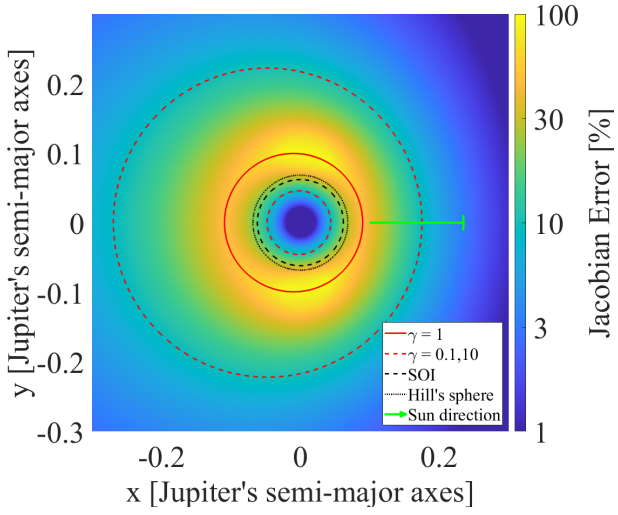

Figure 2: Jupiter's Jacobian percent error (color scale), compared against Hill's surfaces (dotted), SOI (dashed), and analytical loci of points (red).

The "critical" spheroid (parametrised by $\gamma = 1$) can be used as robust flyby detection criterion, assessing if and when a propagation crosses that boundary,

aiming to the minimisation of the truncation error introduced by the interrupted integration. In fact, for the Sun-Earth case this distance falls within the minimum error range identified by Amato et al. [1].

5 Visualisation in the CR3BP

The CR3BP provides further insight on the nature of the thickened regions observed in Figures 1 and 2. Figure 3 shows the perfect alignment of the zero-velocity surfaces, plotted as grey/shadowed areas, with the Jacobian error, on the plane containing Jupiter's orbit about the Sun. The red lines represent different values of γ, equal to 1 (solid), 0.1 or 10 (dotted) and 0.01 (dashed). The selected Jacobi constant to plot the zero-velocity surfaces was only chosen to highlight their alignment with the thickened regions, without particular meaning. On the zero-velocity curves the kinetic energy content of the test particle, the centrifugal reaction due to the non-inertial rotating frame, and the gravitational attraction of both bodies all balance out. Simplifying the dynamical model along this curves may become inaccurate, particularly if close to the Hill sphere boundaries, as highlighted by the thickened error regions. In other words, the mutual effect of the two bodies on how the dynamics changes is more prominent along the zero-velocity surface direction, on a wider region than the sole "critical spheroid".

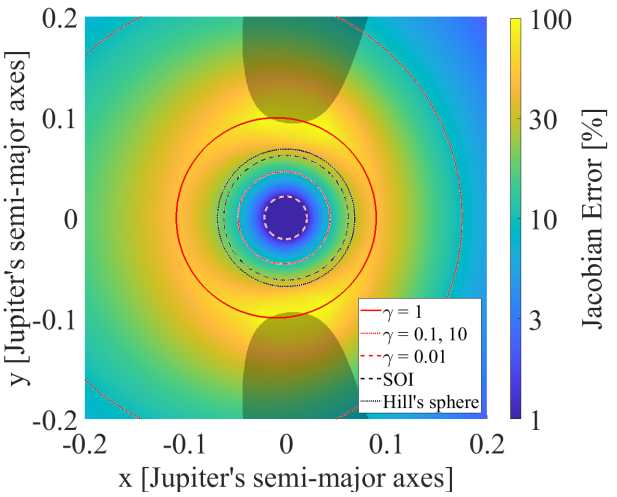

Figure 3: Jupiter's Jacobian percent error (color scale), compared against Hill's surfaces (dotted), SOI (dashed), analytical loci of points (red), and zero-velocity surfaces (grey/shadowed).

6 Conclusion

This work proposes a flyby characterisation approach that accounts for the dynamical nature of the encounter, focussing on the changes on the dynamics caused by the body flown by. The actual smooth transition of the motion from interplanetary to planetary is also modelled, highlighting regions of space where none of the two body is clearly dominating, and approximating the dominance that each body has in each point of the planet neighbourhood.

Apart from the regions nearby the critical distance and along the zero-velocity curves, the proposed parametric analytical model accurately predicts the loci of points of common Jacobian error. Setting the parameter equal to 1 allows the use of the "critical" spheroid as robust flyby detection criterion. Additionally, future works will analyse whether this criterion is also a suitable approach to improve the characterisation of shallow encounters.

Deeper details on the model will be given in the oral presentation, as well as further insight on the comparison with the CR3BP regime and the relation with zero-acceleration saddle points.

Acknowledgments

The research leading to these results has received funding from the European Research Council (ERC) under the European Union's Horizon2020 research and innovation programme as part of project COMPASS (Grant agreement No 679086), `www.compass.polimi.it`, and the European Space Agency (ESA) through the Open Space Innovation Platform (OSIP) co-funded research project "Robust trajectory design accounting for generic evolving uncertainties", Contract No. 4000135476/21/NL/GLC/my.

References

[1] Davide Amato, Giulio Baù, and Claudio Bombardelli. Accurate orbit propagation in the presence of planetary close encounters. *Monthly Notices of the Royal Astronomical Society*, 470(2):2079–2099, Sep 2017.

[2] Frank Debatin, A. Tilgner, and Friedhelm Hechler. Fast numerical integration of interplanetary orbits. In *ESA Special Publication*, volume 255 of *ESA Special Publication*, pages 329–333, Dec 1986.

[3] W.D. McClain and D.A. Vallado. *Fundamentals of Astrodynamics and Applications*. Space Technology Library. Springer Netherlands, 2001.

[4] A Quarteroni, R Sacco, and F Saleri. *Numerical Mathematics Texts in Applied Mathematics*. 2007.

[5] Matteo Romano. *Orbit propagation and uncertainty modelling for planetary protection compliance verification*. PhD thesis, Politecnico di Milano, Supervisors: Colombo, Camilla and Sánchez Pérez, José Manuel, Feb 2020.